6-29-2008

A New Method to Integrate (2+1)-Wave Equations with Dirac's Delta Functions as Sources

Carlos O. Lousto
Rochester Institute of Technology

Hiroyuki Nakano
Rochester Institute of Technology

Recommended Citation
Carlos O Lousto and Hiroyuki Nakano 2008 Class. Quantum Grav. 25 145018

A new method to integrate (2+1)-wave equations with Dirac's delta functions as sources

Carlos O. Lousto and Hiroyuki Nakano

Center for Computational Relativity and Gravitation, School of Mathematical Sciences, Rochester Institute of Technology, Rochester, New York 14623, USA

E-mail: colsma@rit.edu, hxnsma@rit.edu

Abstract. Unlike in the Schwarzschild black hole background, gravitational perturbations in a Kerr black hole background can not be decomposed into simple tensor harmonics in the time domain. Here, we make mode decompositions only in the azimuthal direction. As a first step, we discuss the resulting (2+1)-dimensional Klein-Gordon differential equation for scalar perturbations with a two dimensional Dirac's δ-function as a source representing a point particle orbiting a much larger black hole. To make this equation amenable for numerical integrations we explicitly remove analytically the singular behavior of the source and compute a global, well behaved, effective source for the corresponding waveform.

PACS numbers: 04.25.Nx, 04.70.Bw

Submitted to: *Class. Quantum Grav.*

1. Introduction

One of the main astrophysical targets of LISA [1], a space-based interferometric gravitational wave detector, is the gravitational waves generated by the inspiral of compact objects into massive black holes. To extract physical information of such extreme mass ratio inspirals (EMRI), it is important to know the theoretical gravitational waveforms with sufficient accuracy. For the EMRI scenario, we use the black hole perturbation approach to compute waveforms. Here the compact object is approximated by a point particle orbiting a massive Kerr black hole. In order to obtain the precise theoretical gravitational waveforms we need to solve the self-force problem [2, 3, 4] and then for second order perturbations [5, 4].

It has already been over two years that numerical relativity produced one of the most spectacular breakthroughs in science [6, 7, 8], succeeding in solving the two body problem in general relativity after decades of effort. Among the notable set of results, the discovery [9] of large recoil velocities (up to $4000\,km/s$) [10] stands out. Notably in Ref. [9] a generic binary black hole case was treated, with unequal spins and unequal masses (mass ratio 1/2). It has been hard to deal with extreme mass ratios and recent computations limit to $m_1/m_2 = 3/8$ [11] for spinning holes and up to nearly 1/4 for nonspinning holes [12]. It is foreseeable that soon mass ratios of nearly 1/10 can be achieved in this full numerical simulations making possible a comparison with the semi-analytic approach of the self-force.

The self force problem was formally resolved over ten years ago [13, 14], but its implementation in explicit computations proved lengthy and difficult. This have been reformulated in a more elaborated way by Detweiler and Whiting [15]. The first corrections to the trajectory of an EMRI was computed in [16] for a headon collision using the Regge-Wheeler gauge and the ζ-function regularization. Those results were later confirmed using the standard formalism [17, 18, 19] in the Lorenz gauge [20]. In order to compute the generic orbit corrections around a Schwarzschild black hole, Barack and Lousto [21] have approached the problem of directly solving the linearized Einstein equations in the Lorenz gauge instead of the Regge-Wheeler and Zerilli wave equations [22]. To do that, one needs to be able to develop an accurate algorithm to integrate ten coupled wave-like equations with sources proportional to a Dirac's delta. This algorithm has been developed [23, 24] for the (1+1)-wave equation resulting from the tensor harmonic decomposition of perturbations in the Schwarzschild background, but not for the (2+1)-equation resulting from perturbations of a Kerr (spinning) black hole. This is the subject of the current work.

In this paper, we focus on one aspect of the self-force problem, specifically to derive the full, bare or retarded field of a point source. Therefore, we do not treat the local analysis of the field around the particle's location because the retarded field is global. Here, instead of studying the Teukolsky equation for the curvature perturbations ψ_4, as a first step, we consider the Klein-Gordon equation in the Schwarzschild spacetime, but do not decompose it into spherical harmonics, in order to model perturbations like in

the more generic Kerr background. Recently, introducing a thin worldtube surrounding the worldline of a point particle, Barack and Golbourn [25] have discussed this equation in (2+1)-dimensions as derived by the mode decomposition in the azimuthal direction. A different treatment is proposed here to deal with this problem globally. There is also a method to approximate a Dirac's δ-function by narrow Gaussian [26]. It is, however, difficult to ascertain the error introduced by smearing the particle and if this is accurate enough for self force computations.

Once we obtain the retarded field, each azimuthal mode of the self-force on the particle can be calculated and is finite at the particle location. But the summation over all azimuthal modes diverges. Therefore, we need some regularization to derive the regularized self-force. At this stage, it is necessary to discuss the local analysis of the field or self-force in the derivation of the singular part. The regularized self-force includes two parts, i.e., the conservative part and the dissipative part [27]. To obtain the conservative part of the self-force, we need the regularization, while it is not necessary for the dissipative part which is derived by using a radiative Green's function [28]. Recently, Barack, Golbourn and Sago formulated a new scheme to construct the regularized self force directly from the azimuthal modes of the field in [29].

The paper is organized as follows. In section 2, we discuss the (2+1)-dimensional Klein-Gordon differential equation with a 2-dimensional δ-function as a source. To remove the δ-function, we introduce a new wave-function. This formulation is done in the case of general orbits in the Schwarzschild background. In section 3, we apply the formulation given in section 2 to the case of circular orbits. Here, we obtain a global effective source which is well behaved everywhere. To do so, we also treat boundary behaviors both near the black hole horizon and at spatial infinity. In section 4, we summarize the results of this paper and discuss its applications. Some details of the calculations are given in the appendices. Throughout this paper, we use units in which $c = G = 1$.

2. Formulation

When we calculate the (2+1)-dimensional equation derived from the 4-dimensional Klein-Gordon equation by the azimuthal mode decomposition, the resulting equation is not exactly same as the (2+1)-dimensional wave equation. In our formulation, it is important to derive a differential operator which is the (2+1)-dimensional d'Alambertian of the flat spacetime. By transforming the scalar field, we can obtain an equation which includes the flat (2+1)-dimensional d'Alambertian and a remainder as in (9) below. Then, we remove the 2-dimensional δ-function in the source term by using the Green's function method.

In order to obtain the flat d'Alambertian, we consider the Schwarzschild metric in the isotropic coordinates,

$$ds^2 = -\frac{(2\rho - M)^2}{(2\rho + M)^2}dt^2 + \left(1 + \frac{M}{2\rho}\right)^4 \left[d\rho^2 + \rho^2\left(d\theta^2 + \sin^2\theta d\phi^2\right)\right] . \qquad (1)$$

This radial coordinate is related to that of the Schwarzschild, r,

$$\rho = \frac{r - M + (r^2 - 2Mr)^{1/2}}{2} \,. \tag{2}$$

In the above coordinates, the Klein-Gordon equation with a point source reads

$$\begin{aligned}
&\left[-\frac{(2\,\rho + M)^2}{(2\,\rho - M)^2}\partial_t^2 + \frac{16\rho^4}{(2\,\rho + M)^4}\partial_\rho^2 + \frac{128\rho^5}{(2\,\rho - M)\,(2\,\rho + M)^5}\partial_\rho \right. \\
&\qquad \left. + \frac{16\rho^2}{(2\,\rho + M)^4}\left(\partial_\theta^2 + \cot\theta\partial_\theta + \frac{1}{\sin^2\theta}\partial_\phi^2 \right) \right] \times \psi(t,\rho,\theta,\phi) \\
&\qquad = -q\int_{-\infty}^{\infty} d\tau \frac{64\rho^4 \delta(t - t_z(\tau))\delta(\rho - \rho_z(\tau))\delta(\theta - \theta_z(\tau))\delta(\phi - \phi_z(\tau))}{(2\rho - M)(2\rho + M)^5 \sin\theta} \,,
\end{aligned} \tag{3}$$

where ψ and q denote a scalar field and a scalar charge, respectively. $z^\alpha(\tau)$ is the particle's trajectory with a proper time τ. Here, we use the azimuthal mode decomposition,

$$\psi(t,r,\theta,\phi) = \sum_{m=-\infty}^{\infty} \psi_m(t,\rho,\theta)\exp(im\phi) \,, \tag{4}$$

and then obtain the wave equation for each m mode as

$$\begin{aligned}
&\left[-\frac{(2\,\rho + M)^2}{(2\,\rho - M)^2}\partial_t^2 + \frac{16\rho^4}{(2\,\rho + M)^4}\partial_\rho^2 + \frac{128\rho^5}{(2\,\rho - M)\,(2\,\rho + M)^5}\partial_\rho \right. \\
&\qquad \left. + \frac{16\rho^2}{(2\,\rho + M)^4}\left(\partial_\theta^2 + \cot\theta\partial_\theta - \frac{m^2}{\sin^2\theta} \right) \right] \psi_m(t,\rho,\theta) \\
&\qquad = -q\int_{-\infty}^{\infty} d\tau \frac{64\rho^4 \delta(t - t_z(\tau))\delta(\rho - \rho_z(\tau))\delta(\theta - \theta_z(\tau))}{(2\rho - M)(2\rho + M)^5 \sin\theta} \exp[-im\phi_z(\tau)] \,.
\end{aligned} \tag{5}$$

For the above equation, we transform the field ψ_m as

$$\psi_m(t,\rho,\theta) = 2\left[\frac{\rho}{(2\,\rho + M)\,(2\,\rho - M)\sin\theta} \right]^{1/2} \chi_m(t,\rho,\theta) \,. \tag{6}$$

Above, we have set the radial and angular factors to obtain the spatial part of the flat (2+1)-dimensional d'Alambertian. Then, χ_m satisfies the following equation

$$\begin{aligned}
&\left\{ -\frac{1}{16}\frac{(2\rho + M)^6}{(2\rho - M)^2\rho^4}\partial_t^2 + \partial_\rho^2 + \frac{1}{\rho}\partial_\rho \right. \\
&\qquad \left. + \frac{1}{\rho^2}\left[\partial_\theta^2 - \frac{1}{\sin^2\theta}\left(m^2 - \frac{1}{4}\frac{(4\rho^2 + M^2)^2 - 16\rho M\cos^2\theta}{(2\rho + M)^2(2\rho - M)^2} \right) \right] \right\} \chi_m(t,\rho,\theta) \\
&\qquad = -q\int_{-\infty}^{\infty} d\tau \frac{2\,\delta(t - t_z(\tau))\delta(\rho - \rho_z(\tau))\delta(\theta - \theta_z(\tau))}{[(2\rho - M)(2\rho + M)\rho\sin\theta]^{1/2}} \exp[-im\phi_z(\tau)] \,.
\end{aligned} \tag{7}$$

Note that from the relation $\psi_m \sim \chi_m/\rho^{1/2}$, the source term for χ_m becomes $\rho^{1/2}$ times that for ψ_m. This fact will be used in section 3. Next, we define a new time coordinate

$$T = \int^t dt \, \frac{4\,(2\rho_z(t) - M)\rho_z(t)^2}{(2\rho_z(t) + M)^3} \,, \tag{8}$$

where ρ_z is obtained by solving the geodesic equation and we use the fact that the proper time τ and the argument t in ρ_z are also related by the geodesic equation. From this,

we derive an equation which can be divided into the (2+1)-dimensional d'Alambertian of the flat case $\Box^{(2+1)}$ and a remainder.

$$\begin{aligned}\mathcal{L}_m\,\chi_m(T,\rho,\theta) &= \left(\Box^{(2+1)} + \mathcal{L}_m^{rem}\right)\chi_m(T,\rho,\theta)\\ &= S_m(T,\rho,\theta)\,,\end{aligned} \tag{9}$$

where the differential operators are given by

$$\Box^{(2+1)} = -\partial_T^2 + \partial_\rho^2 + \frac{1}{\rho}\partial_\rho + \frac{1}{\rho^2}\partial_\theta^2\,,$$

$$\begin{aligned}\mathcal{L}_m^{rem} = &\left[1 - \frac{(2\rho_z(T)-M)^2\rho_z(T)^4(2\rho+M)^6}{(2\rho_z(T)+M)^6(2\rho-M)^2\rho^4}\right]\partial_T^2\\ &-\frac{2(4\rho_z(T)-M)(2\rho_z(T)-M)(2\rho+M)^6\rho_z(T)^3M}{(2\rho_z(T)+M)^7(2\rho-M)^2\rho^4}\left(\frac{d\rho_z(T)}{dT}\right)\partial_T\\ &-\frac{1}{\rho^2\sin^2\theta}\left[m^2 - \frac{1}{4}\frac{(4\rho^2+M^2)^2 - 16\rho M\cos^2\theta}{(2\rho+M)^2(2\rho-M)^2}\right]\,,\end{aligned} \tag{10}$$

and the source term is shown to be

$$S_m(T,\rho,\theta) = -q\int_{-\infty}^{\infty} d\tau \frac{2\,\delta(t(T)-t_z(\tau))\delta(\rho-\rho_z(\tau))\delta(\theta-\theta_z(\tau))}{[(2\rho-M)(2\rho+M)\rho\sin\theta]^{1/2}}\exp[-im\phi_z(\tau)]\,. \tag{11}$$

Here, it is noted that there is no ρ and θ derivatives in $\mathcal{L}_m^{rem}$ of (10) because all ρ and θ derivatives are included in $\Box^{(2+1)}$.

To remove the δ-function in the source term, we set

$$\chi_m(T,\rho,\theta) = \chi_m^S(T,\rho,\theta) + \chi_m^{rem}(T,\rho,\theta)\,, \tag{12}$$

where we define the new functions, χ_m^S and χ_m^{rem} as calculated from

$$\Box^{(2+1)}\chi_m^S(T,\rho,\theta) = S_m(T,\rho,\theta)\,, \tag{13}$$

$$\begin{aligned}\mathcal{L}_m\,\chi_m^{rem}(T,\rho,\theta) &= -\mathcal{L}_m^{rem}\chi_m^S(T,\rho,\theta)\\ &= S_m^{(eff)}(T,\rho,\theta)\,.\end{aligned} \tag{14}$$

The effective source $S_m^{(eff)}$ contains no δ-function ‡. Note that $\mathcal{L}_m^{rem}$ includes a second-order derivative. But, since the factor of ∂_T^2 is zero at the particle location, the singular behavior of the effective source $S_m^{(eff)}$ weakens.

The derivation of the singular field χ_m^S can be performed through the Green's function of the (2+1)-dimensional flat case,

$$G(T,\mathbf{x};T',\mathbf{x}') = \frac{1}{2\pi}\frac{1}{[(T-T')^2 - |\mathbf{x}-\mathbf{x}'|^2]^{1/2}}\theta((T-T') - |\mathbf{x}-\mathbf{x}'|)\,, \tag{15}$$

where θ denotes the Heaviside step function, $\mathbf{x}$ is a 2-dimensional spatial vector and the spatial distance is defined by

$$|\mathbf{x}-\mathbf{x}'| = \left[\rho^2 + \rho'^2 - 2\,\rho\,\rho'\cos(\theta-\theta')\right]^{1/2}\,. \tag{16}$$

‡ This decomposition of χ_m does not have any physical-meaning, i.e., χ_m^S is not identified as the singular part to be removed in the self-force calculation. The physically and mathematically-meaningful singular part of the field which is called as the S-part, have been discussed in [15]. Recently, Vega and Detweiler [30] have discussed a new method to derive the retarded field by using a specific approximation to the S-part.

Some detail on the above Green's function is discussion in section Appendix A. Next, χ_m^S is calculated by the following integral

$$\chi_m^S(T,\rho,\theta) = \int dT'\rho' d\rho' d\theta'\, G(T,\mathbf{x};T',\mathbf{x}')S_m(T',\rho',\theta')\,. \tag{17}$$

Here, it should be noted that the Green's function in the above multiple integration is given by analytically. Therefore, it is easy to perform the integration in (17) even for general orbits.

As for the remaining field χ_m^{rem}, we use numerical integrations. However, the effective source $S_m^{(eff)}$ is not amenable for direct numerical integrations due to its non-continuous behavior at the particle location. To explicitly obtain a source term well behaved everywhere, we will apply the formulation discussed above to the case of a particle on a circular orbit.

3. Circular Orbit Case

We consider a particle in a circular orbit given by

$$z^\alpha(\tau) = \left\{u^t\tau,\, r_0,\, \frac{\pi}{2},\, u^\phi\tau\right\}\,, \tag{18}$$

where r_0 denotes the orbital radius in Schwarzschild coordinates. The four velocity u^α is written by

$$u^t = \left(\frac{r_0}{r_0-3M}\right)^{1/2}\,, \quad u^\phi = \left[\frac{M}{r_0^2(r_0-3M)}\right]^{1/2}\,. \tag{19}$$

The relationship between the new time coordinate T and the Schwarzschild time t can be obtained analytically

$$T = \frac{4\,(2\rho_0-M)\rho_0^2}{(2\rho_0+M)^3}\,t\,, \tag{20}$$

where

$$\rho_0 = \frac{r_0 - M + (r_0^2-2Mr_0)^{1/2}}{2}\,. \tag{21}$$

Note that in general, for non circular orbits, we need a numerical integration to derive this relationship.

In order to calculate the singular field, the Green's function in (15) is rewritten in terms of t as

$$\begin{aligned} G(T(t),\mathbf{x};T(t'),\mathbf{x}') = \frac{1}{2\pi}&\frac{1}{\left[\frac{16\,(2\rho_0-M)^2\rho_0^4}{(2\rho_0+M)^6}(t-t')^2 - |\mathbf{x}-\mathbf{x}'|^2\right]^{1/2}} \\ &\times\theta\left(\frac{4\,(2\rho_0-M)\rho_0^2}{(2\rho_0+M)^3}(t-t') - |\mathbf{x}-\mathbf{x}'|\right)\,. \end{aligned} \tag{22}$$

In the following, we will discuss the $m=0$ and $m\neq 0$ modes separately.

The effective source for a final regularized function χ_m^{reg} must go like $\mathrm{O}(\rho^{-2})$ for $\rho\to\infty$ in the case of the $m=0$ mode and $\mathrm{O}(\rho^{-3/2})$ for the $m\neq 0$ mode. The reason

is the following. First, for $\rho \to \infty$, there are only $\rho^{n/2}$ (n: integer) and $\ln \rho$ terms in the effective source of this paper. And, in practice, we will calculate the regularized function of the original field ψ_m numerically. This means that the source term which we will use in the numerical calculation, becomes the factor $\sim 1/\rho^{1/2}$ times the source for χ_m^{reg}. Thus, since we integrate the second order differential equation of (5), we need the above integrability conditions. In a similar manner, at the black hole horizon, i.e., $\rho \to M/2$, the source for ψ_m^{reg} should vanish, i.e., the behavior of the source for χ_m^{reg} should be a power of $(\rho - M/2)$ greater than $1/2$ because the source for ψ_m is the factor $\sim (\rho - M/2)^{-1/2}$ times the source for χ_m^{reg}.

3.1. The $m = 0$ modes

3.1.1. Singular field In the Schwarzschild background, the source term in (11) is time-independent,

$$S_0(t, r, \theta) = -q \frac{2}{u^t \left[(2\rho_0 - M)(2\rho_0 + M)\rho_0\right]^{1/2}} \delta(\rho - \rho_0)\delta(\theta - \pi/2)\,. \tag{23}$$

Therefore, the solution $\chi_0^S(t, r, \theta)$ is obtained from the 2-dimensional Poisson equation as

$$\chi_0^S(t, r, \theta) = -\frac{q}{2\pi} \frac{2\sqrt{\rho_0}}{u^t \left[(2\rho_0 + M)(2\rho_0 - M)\right]^{1/2}} \ln(|\mathbf{x} - \mathbf{x_z}|)\,, \tag{24}$$

where the spatial difference is given by

$$|\mathbf{x} - \mathbf{x_z}| = \left(\rho^2 + \rho_0^2 - 2\,\rho\,\rho_0 \sin\theta\right)^{1/2}\,, \tag{25}$$

In practice, we must normalize the variables inside the logarithmic term in (24). We may take $|\mathbf{x} - \mathbf{x_z}| \to |\mathbf{x} - \mathbf{x_z}|/M$, but we will ignore the factor $1/M$ in the following.

3.1.2. Local behavior The effective source for the $m = 0$ mode, $S_0^{(eff)}$, is calculated by using the solution, χ_0^S, as

$$\begin{aligned} S_0^{(eff)}(t, \rho, \theta) = \frac{q}{8\pi} & \frac{2\sqrt{\rho_0}}{u^t \left[(2\rho_0 + M)(2\rho_0 - M)\right]^{1/2}} \frac{1}{\rho^2 \sin^2\theta} \\ & \times \frac{(4\rho^2 + M^2)^2 - 16\rho^2 M^2 \cos^2\theta}{(2\rho + M)^2(2\rho - M)^2} \ln(|\mathbf{x} - \mathbf{x_z}|)\,. \end{aligned} \tag{26}$$

This effective source is shown in figure 1 for the innermost stable circular orbit ($r_0 = 6M$) case, where $q = 1$, $M = 1$ and $\theta = \pi/2$ §. There is a singular behavior at the particle location. In order to perform the numerical integration with higher accuracy, it is convenient to regularize the source term to be at least C^0 at the particle location.

In order to obtain the source $S_0^{reg,I}$ which is regular at the particle location, we choose the regularization function $\chi_0^{rem,S}$ as

$$\begin{aligned} \chi_0^{rem,S}(t, \rho, \theta) = \frac{q}{16\pi} & \frac{\rho_0^{15/2} \left(2\,\rho - M\right)^3 \left((4\rho^2 + M^2)^2 - 16\rho^2 M^2 \cos^2\theta\right)}{u^t \left(2\,\rho_0 + M\right)^{5/2} \left(2\,\rho_0 - M\right)^{11/2} \rho^9} \\ & \times |\mathbf{x} - \mathbf{x_z}|^2 \ln\left(|\mathbf{x} - \mathbf{x_z}|\right)\,. \end{aligned} \tag{27}$$

§ When we show figures for the $m \neq 0$ mode, we also set $t = 0$ and use the real part of sources.

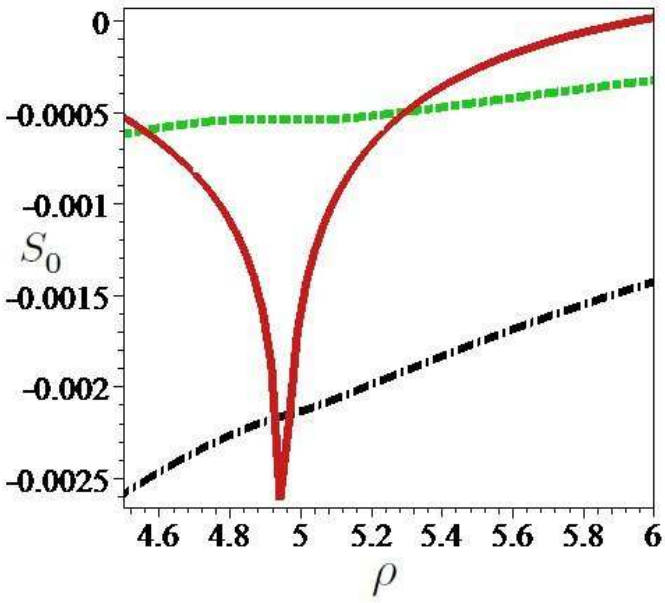

Figure 1. Plot for the $m = 0$ mode of S_m with respect to ρ around the particle location. $S_0^{(eff)}$, $S_0^{reg,I}$, and $S_0^{reg,f}$ are shown by the solid red, dashed green, and dash-dotted black, respectively. The point particle is located at $\rho_0 \sim 4.95$ ($r_0 = 6$).

This regularization function is chosen such that the additional source which arises from this function behaves well both for large ρ and at the horizon. Here, the factors of the power of $1/\rho$ and $(2\rho - M)$ in the above equation give this good behavior. (We will discuss the $m \neq 0$ case by using the same treatment for the regularization function.)

Although this regularization function (and the other regularization functions discussed later) is clearly not unique, the sum of the regularization functions and the regularized function, i.e., the (original) retarded function has the physical-meaning and is unique. This is because the source for the regularized function changes by differences of the regularization functions. Therefore, one may construct any appropriate source by which we can derive a regularized function.

Then, the regularized source at the particle location which is the source for $\chi_0^{rem} - \chi_0^{rem,S}$, is derived as

$$S_0^{reg,I}(t,\rho,\theta) = S_0^{(eff)}(t,\rho,\theta) - \mathcal{L}_0\chi_0^{rem,S}(t,\rho,\theta)\,. \tag{28}$$

We show the above source as the dashed green curve in figure 1. This regular source $S_0^{reg,I}$ behaves as "$x\ln|x|$ for $x \to 0$", i.e., is C^0 around the particle location, and behaves as $\mathrm{O}(1/\rho^2)$ for large ρ (See figure 2.). However, it diverges as $\mathrm{O}(1/(\rho - M/2)^2)$ at the horizon ($\rho = M/2$) (See figure 3.) . Therefore, we need one more regularization at the horizon.

3.1.3. Behavior at the horizon Introducing the regularization function,

$$\chi_0^h(t,\rho,\theta) = \frac{q}{2\,\pi}\frac{\sqrt{\rho_0}}{u^t\left[(2\,\rho_0 - M)\,(2\,\rho_0 + M)\right]^{1/2}\,\rho^2}$$

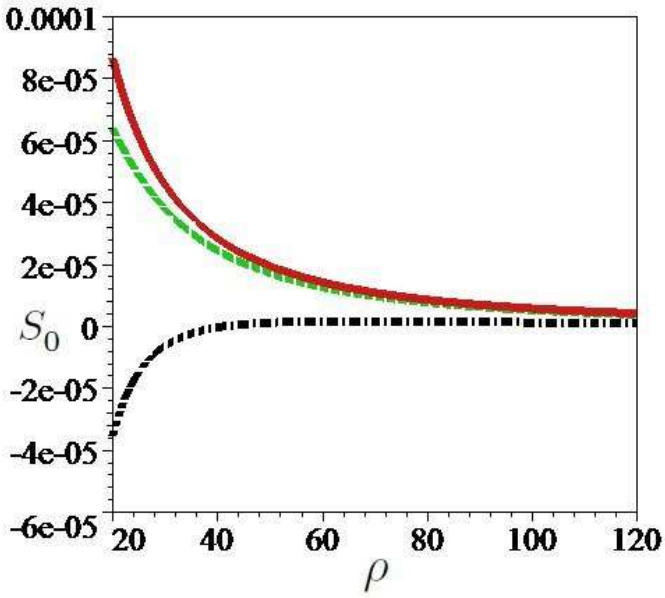

Figure 2. Plot for the $m = 0$ mode of S_m with respect to ρ at large distance. $S_0^{(eff)}$, $S_0^{reg,I}$, and $S_0^{reg,f}$ are shown by the solid red, dashed green, and dash-dotted black, respectively.

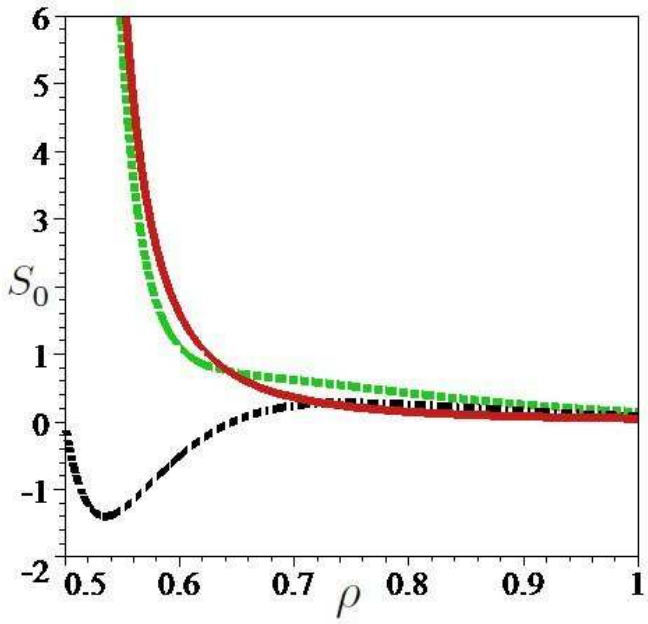

Figure 3. Plot for the $m = 0$ mode of S_m with respect to ρ near the black hole horizon. $S_0^{(eff)}$, $S_0^{reg,I}$, and $S_0^{reg,f}$ are shown by the solid red, dashed green, and dash-dotted black, respectively. The location of the horizon is $\rho = 0.5$.

$$\times\left[\frac{1}{4}\,M^2\,\ln F(\theta) - \frac{M}{F(\theta)}(-M^2\,\ln F(\theta) - 4\,\rho_0^2\,\ln F(\theta) + 4\,\rho_0\,\sin\theta\,M\,\ln F(\theta)\right.$$
$$\left.-M^2 + 2\,\rho_0\,\sin\theta\,M)\left(\rho - \frac{M}{2}\right) - \left(-M^4\,\ln F(\theta) - 24\,M^2\,\rho_0^2\,\ln F(\theta)\right.\right.$$

$$
\begin{aligned}
&+8\,M^3\,\rho_0\,\sin\theta\,\ln F(\theta) - 16\,\rho_0^4\,\ln F(\theta) + 32\,\rho_0^3\,\sin\theta\,M\,\ln F(\theta)\\
&+16\,M^2\,\rho_0^2\,\cos^2\theta\,\ln F(\theta) - 3\,M^4 - 44\,M^2\,\rho_0^2 + 20\,M^3\,\rho_0\,\sin\theta\\
&+32\,\rho_0^3\,\sin\theta\,M + 24\,M^2\,\rho_0^2\,\cos^2\theta\Big)\left(\rho - \frac{M}{2}\right)^2 \Big/ (M^4 + 24\,M^2\,\rho_0^2\\
&-8\,M^3\,\rho_0\,\sin\theta + 16\,\rho_0^4 - 32\,\rho_0^3\,\sin\theta\,M - 16\,M^2\,\rho_0^2\,\cos^2\theta)\Big]\,, \qquad (29)
\end{aligned}
$$

where

$$
F(\theta) = \frac{1}{4}(M^2 + 4\,\rho_0^2 - 4\,\rho_0\,\sin\theta\,M)\,, \qquad (30)
$$

we derive the following source for the regularized function, $\chi_0^{reg} = \chi_0^{rem} - \chi_0^{rem,S} - \chi_0^h$.

$$
S_0^{reg,f}(t,\rho,\theta) = S_0^{reg,I}(t,\rho,\theta) - \mathcal{L}_0\chi_0^h(t,\rho,\theta)\,. \qquad (31)
$$

Here, any bad behavior at infinity does not arise from the above regularization function because we have introduced the factor $1/\rho^2$ in (29). This regularization function have been derived by using the Taylor expansion around the horizon, $\rho = M/2$ (This treatment is also used to derive χ_m^h for $m \neq 0$ in (B.1).) We find that the regularized source is $\mathrm{O}(\rho - M/2)$ as shown by the dash-dotted black curve in figure 1, 2 and 3 and remains of $\mathrm{O}(\rho^{-2})$ for large ρ. This completes the results for the effective source term of the $m = 0$ mode to be used in numerical calculations.

3.2. The $m \neq 0$ modes

3.2.1. Singular field From (17), the singular field for the $m \neq 0$ mode is derived as

$$
\begin{aligned}
\chi_m^S(t,r,\theta) &= \frac{q}{2\pi}\int_{-\infty}^{\infty} d\tau \frac{8\,(2\rho_0 - M)^{1/2}\rho_0^{5/2}}{(2\rho_0 + M)^{7/2}} \frac{\exp(-imu^\phi\tau)}{\left[\frac{16\,(2\rho_0-M)^2\rho_0^4}{(2\rho_0+M)^6}(t - u^t\tau)^2 - |\mathbf{x} - \mathbf{x_z}|^2\right]^{1/2}}\\
&\qquad \times\theta\left(\frac{4\,(2\rho_0 - M)\rho_0^2}{(2\rho_0 + M)^3}(t - u^t\tau) - |\mathbf{x} - \mathbf{x_z}|\right)\\
&= \frac{q}{2\pi}\int_{-\infty}^{T_{ret}} dT_0\,\frac{8\,(2\rho_0 - M)^{1/2}\rho_0^{5/2}}{u^t(2\rho_0 + M)^{7/2}}\\
&\qquad \times\frac{\exp[-im(u^\phi/u^t)T_0]}{\left[\frac{16\,(2\rho_0-M)^2\rho_0^4}{(2\rho_0+M)^6}(t - T_0)^2 - |\mathbf{x} - \mathbf{x_z}|^2\right]^{1/2}}\,, \qquad (32)
\end{aligned}
$$

where the new variable for integration T_0, and the retarded time T_{ret} are defined by

$$
\begin{aligned}
T_0 &= u^t\tau\,,\\
T_{ret} &= t - \frac{(2\rho_0 + M)^3}{4\,(2\rho_0 - M)\rho_0^2}|\mathbf{x} - \mathbf{x_z}|\,. \qquad (33)
\end{aligned}
$$

By introducing the following variable,

$$
\mathcal{T} = \frac{4\,(2\rho_0 - M)\rho_0^2}{(2\rho_0 + M)^3}\,\frac{(t - T_0)}{|\mathbf{x} - \mathbf{x_z}|}\,, \qquad (34)
$$

the above integration can be done as

$$\chi_m^S(t,r,\theta) = \frac{q}{2\pi}\int_1^\infty d\mathcal{T}\frac{2\sqrt{\rho_0}}{u^t\left[(2\rho_0+M)(2\rho_0-M)\right]^{1/2}}\exp(-im\Omega t) \times\frac{\exp\{im\Omega(2\rho_0+M)^3|\mathbf{x}-\mathbf{x_z}|\mathcal{T}/[4\,(2\rho_0-M)\rho_0^2]\}}{\left(\mathcal{T}^2-1\right)^{1/2}} = \frac{i}{4}\,q\,\frac{2\sqrt{\rho_0}\,\exp(-im\Omega t)}{u^t\left[(2\rho_0+M)(2\rho_0-M)\right]^{1/2}}H_0^{(1)}\left(\frac{(2\rho_0+M)^3}{4\,(2\rho_0-M)\rho_0^2}m\Omega|\mathbf{x}-\mathbf{x_z}|\right), \quad (35)$$

where the angular frequency is given by

$$\Omega = \frac{u^\phi}{u^t}, \quad (36)$$

and $H_0^{(1)}$ is the Hankel function of the first kind. The local behavior of the above solution near the particle location is

$$\chi_m^S(t,r,\theta) \sim \chi_m^{SL}(t,r,\theta) = -\frac{q}{2\pi}\frac{2\sqrt{\rho_0}\,\exp(-im\Omega t)}{u^t\left[(2\rho_0+M)(2\rho_0-M)\right]^{1/2}}\ln\left(\frac{(2\rho_0+M)^3}{4\,(2\rho_0-M)\rho_0^2}m\Omega|\mathbf{x}-\mathbf{x_z}|\right). \quad (37)$$

3.2.2. Local behavior When we write the singular field as

$$\chi_m^S = \chi_m^{SL} + \hat{\chi}_m^S, \quad (38)$$

$\hat{\chi}_m^S$ is finite at the particle location. Then, the effective source in (14) becomes

$$S_m^{(eff)}(t,\rho,\theta) = -\frac{q}{2\pi}\frac{2\sqrt{\rho_0}\,\exp(-im\Omega t)}{u^t\left[(2\rho_0+M)(2\rho_0-M)\right]^{1/2}}\ln\left(\frac{(2\rho_0+M)^3}{4\,(2\rho_0-M)\rho_0^2}m\Omega|\mathbf{x}-\mathbf{x_z}|\right) \times\left(-\frac{1}{\rho^2\sin^2\theta}\left(m^2-\frac{1}{4}\frac{(4\rho^2+M^2)^2-16\rho M\cos^2\theta}{(2\rho+M)^2(2\rho-M)^2}\right) -(m\Omega)^2\left(\frac{(2\rho_0+M)^6}{(2\rho_0-M)^2\rho_0^4}-\frac{(2\rho+M)^6}{(2\rho-M)^2\rho^4}\right)\right)-\mathcal{L}_m^{rem}\hat{\chi}_m^S(t,r,\theta), \quad (39)$$

Note that the third line of the above right hand side is at least C^0 at the location of the particle. Therefore, $S_m^{(eff)}$ shown for the $m=1$ mode by the solid red curve in figure 4, has a logarithmic divergence at the particle location. This behavior does not change for each m mode.

To remove the logarithmic divergence in the source, we introduce

$$\chi_m^{rem,S}(t,\rho,\theta) = -\frac{q}{16\pi}|\mathbf{x}-\mathbf{x_z}|^2\ln\left(\frac{(2\rho_0+M)^3}{4\,(2\rho_0-M)\rho_0^2}m\Omega|\mathbf{x}-\mathbf{x_z}|\right) \times\frac{{\rho_0}^{19/2}\,(2\,\rho-M)^3\,\exp(-im\Omega\,t)}{u^t\,(2\,\rho_0+M)^{5/2}\,(2\,\rho_0-M)^{11/2}\,\rho^{11}\sin^2\theta}\left[64\,m^2\rho^4-32\,m^2\rho^2M^2 +4\,m^2M^4+16\,\cos^2\theta\rho^2M^2-(4\rho^2+M^2)^2\right]. \quad (40)$$

Using this regularization function, we obtain a source $S_m^{reg,I}$ for the function $\chi_m^{rem}-\chi_m^{rem,S}$

$$S_m^{reg,I}(t,\rho,\theta) = S_m^{(eff)}(t,\rho,\theta)-\mathcal{L}_m\chi_m^{rem,S}(t,\rho,\theta). \quad (41)$$

The local behavior of $S_m^{reg,I}$, which is shown by the dashed green curve in figure 4, is of the form "$x\ln|x|$ for $x\to 0$", i.e., C^0 at the particle location.

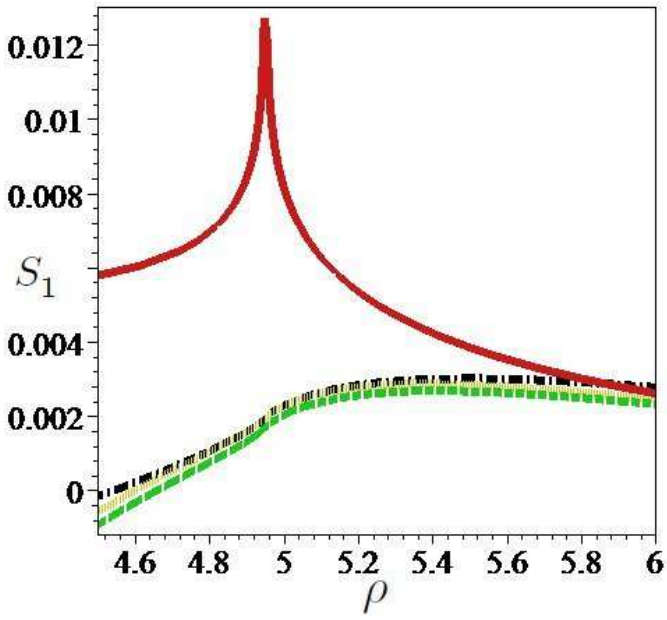

Figure 4. Plot for the $m = 1$ mode of S_m with respect to ρ around the particle location. $S_1^{(eff)}$, $S_1^{reg,I}$, $S_1^{reg,h}$ and $S_1^{reg,f}$ are shown by the solid red, dashed green, dotted yellow and dash-dotted black, respectively. The point particle is located at $\rho_0 \sim 4.95$ ($r_0 = 6$). The $S_1^{reg,I}$, $S_1^{reg,h}$ and $S_1^{reg,f}$ curves have an almost same behavior in this region.

3.2.3. Boundary behavior We now focus on the behavior of the source term at the two boundaries, i.e., at the horizon of the large hole and spatial infinity. (See figure 5 and 6.) To regularize the source at the boundaries, we note that the source contribution from $\chi_m^{rem,S}$ is well behaved. This means that the ill behaviors of the source arise from χ_m^S. Therefore, it is convenient to use the asymptotic behavior of χ_m^S (and some correction factor) for regularization.

For the regularization near the horizon, we use the regularization function χ_m^h given in section Appendix B. Then, the source for the function $\chi_m^{rem} - \chi_m^{rem,S} - \chi_m^h$ becomes

$$S_m^{reg,h}(t,\rho,\theta) = S_m^{reg,I}(t,\rho,\theta) - \mathcal{L}_m\chi_m^h(t,\rho,\theta)\,. \tag{42}$$

This $S_m^{reg,h}$ is shown by the dotted yellow curve in figure 5 and vanishes as $\mathrm{O}(\rho - M/2)$ at the horizon. But this source behaves as $\mathrm{O}(\rho^{-1/2})$ for large ρ. (See figure 6.) To regularize it, we use the regularization function,

$$\chi_m^{\infty}(t,\rho,\theta) = -\left(\frac{2}{\pi}\right)^{1/2} i\,q\,\frac{\rho_0^{3/2}\,\exp(-i\,m\,\Omega\,t)}{u^t\,(2\,\rho_0+M)^2\,(m\,\Omega\,\rho)^{1/2}\,\rho^7}\,(\rho^2+\rho_0^2-2\,\rho_0\,\rho\,\sin\theta)^2$$
$$\times\left(\rho-\frac{M}{2}\right)^3\exp\left[\frac{i}{4}\frac{(2\,\rho_0+M)^3\,m\,\Omega\,(\rho^2+\rho_0^2-2\,\rho_0\,\rho\,\sin\theta)^{1/2}}{(2\,\rho_0-M)\,\rho_0^2}-\frac{i\pi}{4}\right]. \tag{43}$$

The final source for the regularized function $\chi_m^{reg} = \chi_m^{rem} - \chi_m^{rem,S} - \chi_m^h - \chi_m^{\infty}$ becomes

$$S_m^{reg,f}(t,\rho,\theta) = S_m^{reg,h}(t,\rho,\theta) - \mathcal{L}_m\chi_m^{\infty}(t,\rho,\theta)\,. \tag{44}$$

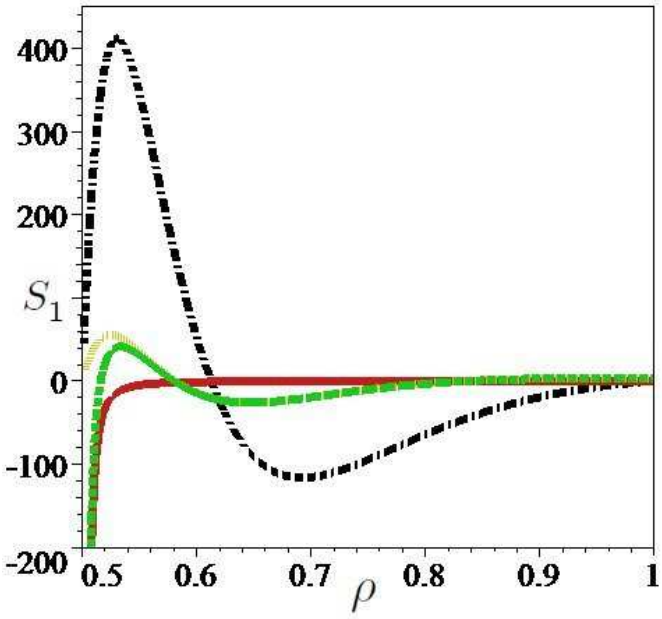

Figure 5. Plot for the $m = 1$ mode of S_m with respect to ρ near the black hole horizon. $S_1^{(eff)}$, $S_1^{reg,I}$, $S_1^{reg,h}$ and $S_1^{reg,f}$ are shown by the solid red, dashed green, dotted yellow and dash-dotted black, respectively. The $S_1^{reg,I}$ and $S_1^{reg,h}$ curves have an almost same behavior except near the horizon. The location of the horizon is $\rho = 0.5$.

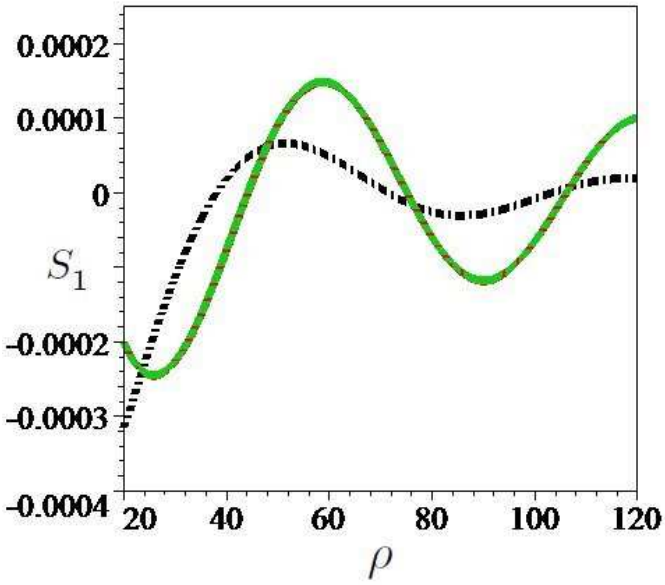

Figure 6. Plot for the $m = 1$ mode of S_m with respect to ρ at large distance. $S_1^{(eff)}$, $S_1^{reg,I}$, $S_1^{reg,h}$ and $S_1^{reg,f}$ are shown by the solid red, dashed green, dotted yellow and dash-dotted black, respectively. The $S_1^{(eff)}$, $S_1^{reg,I}$ and $S_1^{reg,h}$ curves have an almost same behavior in this region.

This $S_m^{reg,f}$ is shown by the dash-dotted black curve in figure 6, and behaves like $\mathrm{O}(\rho^{-3/2}) \times$ (an oscillation factor with respect to ρ) for large ρ. Using this effective

source, we can calculate χ^{reg}_m by numerical calculations.

4. Discussion

In this paper, we have formulated how to derive a global effective source, in replacement of a two-dimensional Dirac's delta, for the (2+1)-dimensional Klein-Gordon differential equation on a black hole background by using a transformation of the scalar field in (6) and a coordinate transformation with respect to time in (8). Here, since we focus on the retarded field which is global, we do not use any local analysis and of the field, but have treated only the fields, i.e., χ^S_m, $\chi^{rem,S}_m$, χ^h_m and χ^∞_m defined globally. The above treatment of the regularization functions is the feature of this paper. On the other hand, Barack and Golbourn [25] have introduced a thin worldtube surrounding the worldline of a point particle, i.e., the local analysis to derive the retarded field. In this approach it is important to obtain results that are insensitive to the choice of the size of the world tube. On the other hand, our approach, determining a global effective source, is straightforward to use, once the regularization is done.

As the application, in the case of circular orbit, we obtained the regularized effective source $S^{reg,f}_m$ for the field χ^{reg}_m. This source is C^0 at the location of the particle, and $\mathrm{O}(\rho - M/2)$ near the horizon. The behavior at infinity is $\mathrm{O}(\rho^{-2})$ for the $m = 0$ mode and $\mathrm{O}(\rho^{-3/2})\times$ (an oscillation factor with respect to ρ) for the $m \neq 0$ modes, which allows straightforward numerical integration.

In the case of general orbits, there is some additional difficulty. If it is possible to use the slow motion approximation and the eccentricity expansion for the bounded orbit cases, we can obtain χ^S_m analytically. Although we need to derive the singular field χ^S_m by numerical calculations in general, these include only the numerical integration for (8) and (17). The regularization functions χ^h_m and χ^∞_m for the field χ^{rem}_m are extracted from the asymptotic behavior directly. This is the same method used in the circular case. About the regularization functions $\chi^{rem,S}_m$, using (17) with the source which is evaluated from the asymptotic behavior of $S^{(eff)}_m$, we can derive $\chi^{rem,S}_m$ by a numerical integration because we need only the most singular part around the particle's location. Hence, there is no trouble to obtain the effective source for χ^{reg}_m.

When we consider the extension of this formulation to the Kerr background case, we can also extract a similar differential operator to that of (9). In practice, we have the (2+1)-dimensional d'Alambertian of the flat spacetime in this case. The mode decomposition only in the azimuthal direction has already been used, therefore, the same treatment discussed in this paper is applicable.

Finally, in the case of gravitational perturbations, we have ten field equations for the linear perturbation in the Lorenz gauge. (See [21].) We can also extract the (2+1)-dimensional d'Alambertian of the flat spacetime from them. The same treatment also holds to those equations. The method can also be used to deal with the Teukolsky differential equation [31] with the corresponding corrections for the presence of not only Dirac's delta but first and second derivatives of it as source terms.

Acknowledgments

We would like to thank N. Sago and H. Tagoshi for useful discussions. This is supported by JSPS for Research Abroad (HN), by the NSF through grants PHY-0722315, PHY-0701566, PHY-0714388, and PHY-0722703, and from grant NASA 07-ATFP07-0158.

Appendix A. About Green's function

To obtain χ^S_m from (13) we use the Green's function method. Here we consider the Green's function in the Cartesian coordinates, i.e., $x = r\cos\theta$ and $y = r\sin\theta$

$$\left(-\partial_t^2 + \partial_x^2 + \partial_y^2\right) G(t, \mathbf{x}; t', \mathbf{x}') = -\delta(t-t')\delta^{(2)}(\mathbf{x}-\mathbf{x}')\,, \tag{A.1}$$

where $\delta^{(2)}$ denotes the 2-dimensional δ-function. A solution of the above equation is usually calculated by using the Fourier transformation,

$$G(t, \mathbf{x}; t', \mathbf{x}') = \frac{1}{2\,\pi}\int_{-\infty}^{\infty} d\omega G_\omega(\mathbf{x}; t', \mathbf{x}')\exp(-i\omega t)\,. \tag{A.2}$$

In the frequency domain, the Green's function satisfies the equation,

$$\left(\omega^2 + \partial_x^2 + \partial_y^2\right) G_\omega(\mathbf{x}; t', \mathbf{x}') = -\exp(i\omega t')\delta^{(2)}(\mathbf{x}-\mathbf{x}')\,. \tag{A.3}$$

The Green's function must become a homogeneous solution of the above equation for $\mathbf{x} \neq \mathbf{x}'$. And, near the singularity, $\mathbf{x} \to \mathbf{x}'$, the Green's function must behave as $G_\omega \sim -1/(2\pi)\ln|\mathbf{x}-\mathbf{x}'|$. Furthermore, we need to set a boundary condition. The outgoing boundary condition is used here. From the above three conditions, the Green's function in the frequency domain is obtained as

$$G_\omega(\mathbf{x}; t', \mathbf{x}') = \frac{i}{4}H_0^{(1)}(\omega|\mathbf{x}-\mathbf{x}'|)\exp(i\omega t')\,, \tag{A.4}$$

where $H_0^{(1)}$ is the Hankel functions of the first kind.

We go back to the time domain by using (A.2).

$$G(t, \mathbf{x}; t', \mathbf{x}') = \frac{i}{8\pi}\int_{-\infty}^{\infty} H_0^{(1)}(\omega|\mathbf{x}-\mathbf{x}'|)\exp[-i\omega(t-t')]\,. \tag{A.5}$$

Note that $H_0^{(1)}(-|\omega||\mathbf{x}-\mathbf{x}'|) = -H_0^{(2)}(|\omega||\mathbf{x}-\mathbf{x}'|)$. Here, we use an integral representation of the Hankel functions

$$\begin{aligned} H_0^{(1)}(x) &= \frac{-2i}{\pi}\int_1^\infty dt \frac{\exp(ixt)}{(t^2-1)^{1/2}}\,, \\ H_0^{(2)}(x) &= \frac{2i}{\pi}\int_1^\infty dt \frac{\exp(-ixt)}{(t^2-1)^{1/2}}\,, \end{aligned} \tag{A.6}$$

and then, the Green's function in the time domain is derived as

$$G(t, \mathbf{x}; t', \mathbf{x}') = \frac{1}{2\pi}\frac{1}{\left[(t-t')^2 - |\mathbf{x}-\mathbf{x}'|^2\right]^{1/2}}\theta((t-t') - |\mathbf{x}-\mathbf{x}'|)\,. \tag{A.7}$$

From the above Heaviside step function, this Green's function has support not only on the light cone, but also inside the light cone. This is mentioned as a failure of the Huygens principle [32]. This feature of the Green's function has been discussed in Refs. [33, 32, 34]. The above Green's function is also derived from the direct integration of the (3+1)-dimensional Green's function with respect to the axial direction [33].

Appendix B. Regularization function, χ_m^h

The function χ_m^h for the regularization near the horizon is so long that we summarize it in this appendix.

$$\chi_m^h(t,\rho,\theta) = \frac{-1}{32}\, i\, q\, \frac{\sqrt{\rho_0}\, M^4}{u^t\, [(2\,\rho_0 - M)\,(2\,\rho_0 + M)]^{1/2}\ \rho^4}\ \exp(-i\, m\, \Omega\, t)$$
$$\times\Bigg\{ C_0(\rho,\,\theta) H_0^{(1)}\left[\frac{(2\rho_0+M)^3}{4\,(2\rho_0-M)\rho_0^2} m\Omega\sqrt{F(\theta)}\right]$$
$$+C_1(\rho,\,\theta) H_1^{(1)}\left[\frac{(2\rho_0+M)^3}{4\,(2\rho_0-M)\rho_0^2} m\Omega\sqrt{F(\theta)}\right]$$
$$+C_2(\rho,\,\theta) H_2^{(1)}\left[\frac{(2\rho_0+M)^3}{4\,(2\rho_0-M)\rho_0^2} m\Omega\sqrt{F(\theta)}\right]\Bigg\}, \tag{B.1}$$

where

$$C_0(\rho,\,\theta) = 1 + \frac{8}{M}\left(\rho - \frac{M}{2}\right) - \frac{1}{64}\Big[64\, M^4\, m^4\, (2\,\rho_0 + M)^6 (M^4 + 12\, M^2\, \rho_0^2\, \cos^2\theta$$
$$-8\, M^2\, \rho_0^2 - 16\, M\, \cos^2\theta\, \rho_0^3\, \sin\theta - 16\, \rho_0^4\, \cos^2\theta + 16\, \rho_0^4)\Omega^4$$
$$+M^2\, m^2 (29376\, M^5\, \rho_0^5\, \cos^2\theta + 2448\, M^7\, \rho_0^3\, \cos^2\theta - 6274048\, \rho_0^{10}$$
$$+884\, M^8\, \rho_0^2 + 17\, M^{10} - 3264\, M^6\, \rho_0^4\, \cos^2\theta\, \sin\theta - 43520\, M^4\, \cos^2\theta\, \rho_0^6\, \sin\theta$$
$$-3128320\, \rho_0^7\, M^3 + 204\, M^8\, \rho_0^2\, \cos^2\theta - 52224\, M\, \rho_0^9\, \cos^2\theta$$
$$-52224\, M^2\, \rho_0^8\, \sin\theta\, \cos^2\theta + 1088\, M^7\, \rho_0^3 - 16320\, M^5\, \rho_0^5\, \cos^2\theta\, \sin\theta$$
$$+204\, \rho_0\, M^9 - 17408\, \rho_0^{10}\, \cos^2\theta - 17408\, M\, \rho_0^9\, \sin\theta\, \cos^2\theta$$
$$-65280\, M^3\, \rho_0^7\, \sin\theta\, \cos^2\theta - 272\, M^7\, \rho_0^3\, \cos^2\theta\, \sin\theta + 377984\, \rho_0^5\, M^5$$
$$-6343680\, M^2\, \rho_0^8\, \cos^2\theta - 1540224\, M^4\, \rho_0^6\, \cos^2\theta + 6343680\, M\, \rho_0^9$$
$$+6287104\, M^3\, \rho_0^7\, \cos^2\theta + 11968\, M^6\, \rho_0^4\, \cos^2\theta + 1629440\, M^2\, \rho_0^8$$
$$+377984\, M^4\, \rho_0^6 - 102112\, M^6\, \rho_0^4)\Omega^2 - 13824\, \rho_0^4\, (2\,\rho_0 - M)^2 (M^4$$
$$+16\, M^2\, \rho_0^2\, \cos^2\theta - 8\, M^2\, \rho_0^2 + 16\, \rho_0^4)\Big]\left(\rho - \frac{M}{2}\right)^2 \Big/ \Big[(2\,\rho_0 - M)^2$$
$$\times(9 + 64\, M^2\, m^2\, \Omega^2)\, \rho_0^4\, M^2 (M^4 + 16\, M^2\, \rho_0^2\, \cos^2\theta - 8\, M^2\, \rho_0^2 + 16\, \rho_0^4)\Big],$$

$$C_1(\rho,\,\theta) = \frac{1}{4}(2\,\rho_0 + M)^3\, \Omega\, m (M^9 - 18\, \rho_0\, M^8\, \sin\theta - 128\, M^7\, \rho_0^2\, \cos^2\theta + 144\, \rho_0^2\, M^7$$
$$+448\, \rho_0^3\, M^6\, \sin\theta\, \cos^2\theta - 672\, M^6\, \rho_0^3\, \sin\theta + 768\, M^5\, \rho_0^4\, \cos^4\theta$$
$$-2688\, M^5\, \rho_0^4\, \cos^2\theta + 2016\, M^5\, \rho_0^4 - 4032\, \rho_0^5\, M^4\, \sin\theta + 5376\, \rho_0^6\, M^3$$
$$+3584\, \rho_0^5\, M^4\, \sin\theta\, \cos^2\theta - 512\, \rho_0^5\, M^4\, \sin\theta\, \cos^4\theta - 7168\, \rho_0^6\, M^3\, \cos^2\theta$$
$$+2048\, \rho_0^6\, M^3\, \cos^4\theta + 3072\, \rho_0^7\, M^2\, \sin\theta\, \cos^2\theta - 4608\, \rho_0^7\, M^2\, \sin\theta$$
$$+2304\, \rho_0^8\, M - 2048\, \rho_0^8\, M\, \cos^2\theta - 512\, \rho_0^9\, \sin\theta)\left(\rho - \frac{M}{2}\right)$$
$$\Big/\Big[(M^2 + 4\,\rho_0^2 - 4\,\rho_0\, \sin\theta\, M)^{9/2} \rho_0^2\, (-2\,\rho_0 + M)\Big]$$
$$+\Big[64\, M^2\, m^2 (2\, M^9 + 288\, \rho_0^2\, M^7 + 7008\, \rho_0^5\, M^4\, \sin\theta\, \cos^2\theta + 10752\, \rho_0^6\, M^3$$

$$
\begin{aligned}
&-14096\,\rho_0^6\,M^3\,\cos^2\theta - 8064\,\rho_0^5\,M^4\,\sin\theta + 4032\,M^5\,\rho_0^4 - 1024\,\rho_0^9\,\sin\theta \\
&-9216\,\rho_0^7\,M^2\,\sin\theta - 255\,M^7\,\rho_0^2\,\cos^2\theta + 4608\,\rho_0^8\,M - 1344\,M^6\,\rho_0^3\,\sin\theta \\
&+884\,\rho_0^3\,M^6\,\sin\theta\,\cos^2\theta + 5952\,\rho_0^7\,M^2\,\sin\theta\,\cos^2\theta + 3904\,\rho_0^6\,M^3\,\cos^4\theta \\
&-4032\,\rho_0^8\,M\,\cos^2\theta - 5316\,M^5\,\rho_0^4\,\cos^2\theta - 960\,\rho_0^5\,M^4\,\sin\theta\,\cos^4\theta \\
&+1488\,M^5\,\rho_0^4\,\cos^4\theta - 36\,\rho_0\,M^8\,\sin\theta)\Omega^2 + 16\,M^9 + 2368\,\rho_0^2\,M^7 \\
&+40960\,\rho_0^8\,M + 33600\,\rho_0^6\,M^3\,\cos^4\theta + 59744\,\rho_0^5\,M^4\,\sin\theta\,\cos^2\theta \\
&-80896\,\rho_0^7\,M^2\,\sin\theta - 11200\,M^6\,\rho_0^3\,\sin\theta - 121872\,\rho_0^6\,M^3\,\cos^2\theta \\
&-44804\,M^5\,\rho_0^4\,\cos^2\theta + 52032\,\rho_0^7\,M^2\,\sin\theta\,\cos^2\theta - 35776\,\rho_0^8\,M\,\cos^2\theta \\
&-9216\,\rho_0^9\,\sin\theta + 93184\,\rho_0^6\,M^3 - 8128\,\rho_0^5\,M^4\,\sin\theta\,\cos^4\theta \\
&+7348\,\rho_0^3\,M^6\,\sin\theta\,\cos^2\theta - 68992\,\rho_0^5\,M^4\,\sin\theta + 12496\,M^5\,\rho_0^4\,\cos^4\theta \\
&-292\,\rho_0\,M^8\,\sin\theta - 2095\,M^7\,\rho_0^2\,\cos^2\theta + 34048\,M^5\,\rho_0^4\Big]\,m\,\Omega\,(2\,\rho_0 + M)^3 \\
&\times\left(\rho - \frac{M}{2}\right)^2 \Big/\Big[(-2\,\rho_0 + M)\,M\,\rho_0^2\,(M^2 + 4\,\rho_0^2 - 4\,\rho_0\,\sin\theta\,M)^{9/2} \\
&\times(9 + 64\,M^2\,m^2\,\Omega^2)\Big]\,,
\end{aligned}
$$

$$
\begin{aligned}
C_2(\rho,\,\theta) = \frac{1}{64}&(M^2 - 4\,\rho_0\,\sin\theta\,M + 4\,\rho_0^2 - 4\,\cos^2\theta\,\rho_0^2)\,\Omega^2\,m^2(2\,\rho_0 + M)^6(64\,M^2\,m^2\,\Omega^2 \\
&+1)\,\left(\rho - \frac{M}{2}\right)^2 \Big/\Big[F(\theta)\,(-2\,\rho_0 + M)^2\,\rho_0^4(9 + 64\,M^2\,m^2\,\Omega^2)\Big] \qquad \text{(B.2)}
\end{aligned}
$$

In the above equations, $F(\theta)$ is the same as defined in (30).

References

[1] K. Danzman *et al*, *LISA – Laser Interferometer Space Antenna, Pre-Phase A Report*, Max-Planck-Institute fur Quantenoptic, Report MPQ 233 (1998).

[2] E. Poisson, *General relativity and gravitation. Proceedings of GR17*, 119 (2005) [arXiv:gr-qc/0410127].

[3] W. Hikida, H. Nakano and M. Sasaki, Class. Quant. Grav. **22**, S753 (2005) [arXiv:gr-qc/0411150].

[4] C. O. Lousto (ed.), *Special issue: Gravitational Radiation from Binary Black Holes: Advances in the Perturbative Approach*, Class. Quant. Grav. **22**, S543-S868, (2005).

[5] H. Nakano and C. O. Lousto, arXiv:gr-qc/0701039.

[6] F. Pretorius, Phys. Rev. Lett. **95**, 121101 (2005) [arXiv:gr-qc/0507014].

[7] M. Campanelli, C. O. Lousto, P. Marronetti and Y. Zlochower, Phys. Rev. Lett. **96**, 111101 (2006) [arXiv:gr-qc/0511048].

[8] J. G. Baker, J. Centrella, D. I. Choi, M. Koppitz and J. van Meter, Phys. Rev. Lett. **96**, 111102 (2006) [arXiv:gr-qc/0511103].

[9] M. Campanelli, C. O. Lousto, Y. Zlochower and D. Merritt, Astrophys. J. **659**, L5 (2007) [arXiv:gr-qc/0701164].

[10] M. Campanelli, C. O. Lousto, Y. Zlochower and D. Merritt, Phys. Rev. Lett. **98**, 231102 (2007) [arXiv:gr-qc/0702133].

[11] C. O. Lousto and Y. Zlochower, Phys. Rev. D **77**, 044028 (2008) [arXiv:0708.4048 [gr-qc]].

[12] J. A. Gonzalez, U. Sperhake, B. Bruegmann, M. Hannam and S. Husa, Phys. Rev. Lett. **98**, 091101 (2007) [arXiv:gr-qc/0610154].

[13] Y. Mino, M. Sasaki and T. Tanaka, Phys. Rev. D **55**, 3457 (1997) [arXiv:gr-qc/9606018].
[14] T. C. Quinn and R. M. Wald, Phys. Rev. D **56**, 3381 (1997) [arXiv:gr-qc/9610053].
[15] S. Detweiler and B. F. Whiting, Phys. Rev. D **67**, 024025 (2003) [arXiv:gr-qc/0202086].
[16] C. O. Lousto, Phys. Rev. Lett. **84**, 5251 (2000) [arXiv:gr-qc/9912017].
[17] L. Barack, Y. Mino, H. Nakano, A. Ori and M. Sasaki, Phys. Rev. Lett. **88**, 091101 (2002) [arXiv:gr-qc/0111001].
[18] Y. Mino, H. Nakano and M. Sasaki, Prog. Theor. Phys. **108**, 1039 (2003) [arXiv:gr-qc/0111074].
[19] L. Barack and A. Ori, Phys. Rev. D **67**, 024029 (2003) [arXiv:gr-qc/0209072].
[20] L. Barack and C. O. Lousto, Phys. Rev. D **66**, 061502 (2002) [arXiv:gr-qc/0205043].
[21] L. Barack and C. O. Lousto, Phys. Rev. D **72**, 104026 (2005) [arXiv:gr-qc/0510019].
[22] H. Nakano, N. Sago and M. Sasaki, Phys. Rev. D **68**, 124003 (2003) [arXiv:gr-qc/0308027].
[23] C. O. Lousto and R. H. Price, Phys. Rev. D **56**, 6439 (1997) [arXiv:gr-qc/9705071].
[24] C. O. Lousto, Class. Quant. Grav. **22**, S543 (2005) [arXiv:gr-qc/0503001].
[25] L. Barack and D. A. Golbourn, Phys. Rev. D **76**, 044020 (2007) [arXiv:0705.3620 [gr-qc]].
[26] R. Lopez-Aleman, G. Khanna and J. Pullin, Class. Quant. Grav. **20**, 3259 (2003) [arXiv:gr-qc/0303054].
[27] A. Pound and E. Poisson, Phys. Rev. D **77**, 044013 (2008) [arXiv:0708.3033 [gr-qc]].
[28] Y. Mino, Phys. Rev. D **67**, 084027 (2003) [arXiv:gr-qc/0302075].
[29] L. Barack, D. A. Golbourn and N. Sago, Phys. Rev. D **76**, 124036 (2007) [arXiv:0709.4588 [gr-qc]].
[30] I. Vega and S. Detweiler, arXiv:0712.4405 [gr-qc].
[31] S. A. Teukolsky, Astrophys. J. **185**, 635 (1973).
[32] P. O. Kazinski, S. L. Lyakhovich and A. A. Sharapov, Phys. Rev. D **66**, 025017 (2002) [arXiv:hep-th/0201046].
[33] D. V. Galtsov, Phys. Rev. D **66**, 025016 (2002) [arXiv:hep-th/0112110].
[34] V. Cardoso, O. J. C. Dias and J. P. S. Lemos, Phys. Rev. D **67**, 064026 (2003) [arXiv:hep-th/0212168].